

Decellularized Tissue Matrix Enhances Self-Assembly of Islet Organoids from Pluripotent Stem Cell Differentiation

Huanjing Bi, Soujanya S. Karanth, Kaiming Ye, Roland Stein, and Sha Jin*


Cite This: <https://dx.doi.org/10.1021/acsbiomaterials.0c00088>


Read Online

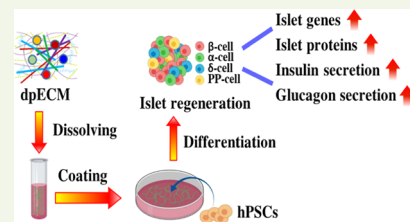
ACCESS |

Metrics & More

Article Recommendations

Supporting Information

ABSTRACT: Regenerating human islet organoids from stem cells remains a significant challenge because of our limited knowledge on cues essential for developing the endocrine organoids *in vitro*. In this study, we discovered that a natural material prepared from a decellularized rat pancreatic extracellular matrix (dpECM) induces the self-assembly of human islet organoids during induced pluripotent stem cell (iPSC) pancreatic differentiation. For the first time, we demonstrated that the iPSC-derived islet organoids formed in the presence of the dpECM are capable of glucose-responsive secretion of both insulin and glucagon, two major hormones that maintain blood glucose homeostasis. The characterization of the organoids revealed that the organoids consisted of all major endocrine cell types, including α , β , δ , and pancreatic polypeptide cells, that were assembled into a tissue architecture similar to that of human islets. The exposure of iPSCs to the dpECM during differentiation resulted in considerably elevated expression of key pancreatic transcription factors such as PDX-1, MAFA, and NKKX6.1 and the production of all major hormones, including insulin, glucagon, somatostatin, and pancreatic polypeptide from stem cell-derived organoids. This study highlights the importance of natural, bioactive biomaterials for building microenvironments crucial to regenerating islet organoids from stem cells.



KEYWORDS: detergent-free decellularization, pancreatic extracellular matrix, human induced pluripotent stem cells, islet organoids, glucagon, insulin

INTRODUCTION

Diabetes is projected to be one of the leading causes of death by 2030. In patients with type 1 diabetes (T1D), the islets of Langerhans not only fail to produce the hormone insulin due to autoimmune destruction of β cells but also secrete the counter regulatory hormone glucagon (GCG) from islet α cells at inappropriate levels.¹ A number of studies have revealed that an abnormal level of GCG secretion from α cells in T1D patients¹ leads to exacerbation of hyperglycemia due to hyperglucagonemia and failed counter-regulation of insulin secretion.² Moreover, the imbalance between insulin and GCG production by β and α cells plays a crucial role in the development of type 2 diabetes (T2D).³ The dysfunction of α cells in the islets is one of the major causes that leads to excessive hepatic glucose production and insulin resistance in T2D patients.^{4,5} Indeed, the heterotypic interactions between human α and β cells is paramount in regulating glucose homeostasis by the islets.^{6–8} It is found that the long-term complications associated with T1D are due to the inability of injected insulin to recapitulate the facile regulation of glucose homeostasis in the same manner as endogenous islet cells. Furthermore, somatostatin (SST) secreted from δ cells is also crucial to balance hormone levels and prevent overproduction of certain hormones.⁹ Pancreatic polypeptide secreted from pancreatic polypeptide (PP) cells is found to be correlated to SST levels in response to eating and fasting.¹⁰ Although human islet transplantation would likely be a promising treatment, the

limited availability of cadaveric donors makes this impractical.^{11–13} Hence, it is highly desired to generate islets that are composed of four different types of endocrine cells, including α , β , δ , and PP cells. This necessity becomes more profound when human islets are needed for drug screening and diabetes pathophysiological study.

Human pluripotent stem cells (hPSCs), which include induced pluripotent stem cells (iPSCs), are promising cell sources for generating pancreatic islets. Although extensive efforts have led to the generation of glucose-responsive, insulin-secreting β cells over the past years,^{12,14–21} the production of islet organoids has had limited success.^{13,22–24} For instance, the cytostructure and cellular composition of these cell clusters are distinct from adult islets.^{23–25} Particularly, islet PP cells were not detected from these islet clusters.^{12,26–28} The islet clusters generated from human umbilical cord mesenchymal stem cells appear to lack δ and PP cells entirely.²⁹ However, it is recognized that paracrine regulation by the various islet hormones is essential for maintaining physiological blood glucose regulation, which is

Received: January 18, 2020

Accepted: May 21, 2020

Published: May 21, 2020

principally mediated through insulin actions on storage, GCG on release, and SST on insulin and GCG secretion. Accordingly, the composition and association of islet cells is expected to have a profound effect on islet function. It is, therefore, of critical importance to develop an approach to guide the self-assembly of endocrine cells to assemble into an architecture that resembles the tissue structure of adult islets from iPSCs.

The development of interspecies pancreata has also been attempted. Yamaguchi et al. have demonstrated that mouse pancreas can be grown in and harvested from a rat host.³⁰ The transplantation of interspecies pancreas in mice reverses diabetes; however, the application of this technology in humans remains challenging. Recently, we have demonstrated that the human islet organoids, consisting all endocrine cells can be generated from hPSCs in a collagen-based scaffold or under type V collagen signaling.^{13,31} The cytostructural analysis of these organoids revealed an architecture typical of human adult islets. Both β cells and non- β cells were mixed randomly to form organoids that secrete insulin in response to glucose challenges. Nevertheless, cues that permit islet organoid development is incomplete. In this study, we aimed to create microenvironments from natural, biological materials for islet development in vitro. We developed a detergent-free decellularization approach to obtain decellularized rat pancreatic extracellular matrix (dpECM) substrates. Using the resultant dpECM substrates as a supplementary tissue specific microenvironment through surface coating, we discovered for the first time that the exposure of hPSCs to dpECM substrates permits the self-organization of islet-like organoids during pancreatic differentiation. These self-assembled organoids consist of α , β , δ , and PP cells, secreting both glucose-regulated insulin and GCG. These findings provide the first evidence of the pancreatic ECM's role in promoting the development of human islet organoids in vitro.

MATERIALS AND METHODS

dpECM Preparation. Rat pancreata were obtained from the Laboratory of Animal Resources at Binghamton University. Male and female Sprague Dawley rats (Charles River) 2 to 12 weeks old were euthanized by CO_2 asphyxiation according to the American Veterinary Medical Association guidelines. Pancreata were isolated, rinsed with cold PBS, and stored at -80°C until use. The frozen pancreata were cut into 1.5 mm sections using a deli-style slicer (Chef's choice 632, EdgeCraft Corporation). The slices were rinsed with deionized water (dH_2O) five times on a tube rotator (Boekel Industries, Inc.) with a speed of 20 rpm at 4°C . The tissues were then divided into the following groups for decellularization. (1) DB1: samples were washed with 1% Triton X-100 (Thermo Fisher Scientific) solution six times, and the solution was changed every 16 h. (2) DB2: samples were washed with 0.5% sodium dodecyl sulfate (SDS) (VWR International, LLC) five times and 1% Triton X-100 solution once. Solutions were changed every 16 h. (3) DF1: samples were washed with dH_2O six times, and water was changed every 16 h. (4) DF2: samples were processed in four cycles with 10% NaCl/ dH_2O washes, that is, gently shaken in 100 g/L sodium chloride solution at 4°C for 12 h, then shaken in dH_2O for another 12 h at 4°C . (5) Samples were processed in four cycles with 10% NaCl + 0.1% NH_4OH / dH_2O washes. All decellularization procedures were aseptically performed at 4°C with gentle shaking. After decellularization, the materials were extensively rinsed with dH_2O by shaking at 4°C for 12 h. The decellularized tissues were lyophilized and comminuted using a Wiley Mini-Mill (Thomas Scientific). To solubilize the dpECM powder, 100 mg of lyophilized dpECM powder was digested by 10 mg of pepsin (Sigma) in 5 mL of 0.02 N acetic acid with continuous stirring at room temperature for

48 h, after which the ECM powder was dissolved with minor or no insoluble fraction. The resultant dpECM solution was aliquoted and stored at -80°C until use. Cytotoxicity of the dpECM was determined using a viability/cytotoxicity kit (Life Technologies) and evaluated under a Nikon Eclipse Ti motorized phase contrast inverted fluorescence microscope.

dpECM Characterization. Decellularized samples were fixed with 4% formaldehyde overnight and cryoprotected with 30% sucrose for 24 h, then embedded in optimal cutting temperature (OCT) for cryo-sectioning. Samples were cut into 10 μm thick sections and hematoxylin and eosin staining (H&E staining) was performed to determine the histological morphology of the dpECM. For scanning electron microscopy (SEM) imaging, Petri dishes coated with either growth factor reduced Matrigel (Corning Life Science, refer to Matrigel thereafter), dpECM, or Matrigel and dpECM mixture were fixed with 2.5% glutaraldehyde in 0.1 M PBS (pH 7.4) for 60 min. The samples were rinsed with PBS followed by dehydrating with gradient series of alcohol for 15 min each. Additionally, samples were critical point dried and carbon coated using a Cressington 208C coater (Cressington Scientific Instruments) to a thickness of >10 nm. Electron microscope images were taken using a Zeiss Supra 55-VP scanning electron microscope using an accelerating voltage of 5 kV. Total deoxyribonucleic acid (DNA) was extracted from a lyophilized dpECM using a DNeasy kit (QIAGEN) and quantified using a Synergy H1 Microplate Reader (BioTek). Proteomics analysis was performed as described in our previous study.³¹ In brief, the dpECM and growth factor-reduced Matrigel were analyzed by liquid chromatography-tandem mass spectrometry (LC-MS/MS) and label-free quantitation by Bioproximity, LLC. Spectra were searched using X!Tandem and OMSSA. Protein identifications were accepted if they were assigned at least two unique validated peptides and had a protein probability of at least 99%.

Islet Organoid Development. Human iPSC line IMR90 and hESC line H9 (WiCell Research Institute) were maintained in mTeSR1 medium (StemCell Technologies), as described in our previous work.^{32,33} For islet organoid development, cells were dissociated with Accutase (StemCell Technologies) and seeded (1×10^6 cells/well) onto Matrigel (M)- or Matrigel+dpECM (M+d)-coated 6-well plates and cultured in mTeSR1 medium. The ratios of M to d in the mixed M+d solution were 4:1 or 2:1 (w/w). For M+d coating, M was diluted to a concentration of 80 $\mu\text{g}/\text{mL}$ in DMEM/F12 (HyClone) with 20 $\mu\text{g}/\text{mL}$ dpECM (4:1) or 40 $\mu\text{g}/\text{mL}$ dpECM (2:1). The mixture was added into culture plates and incubated at 37°C for 1 h before cell seeding. Stepwise differentiation protocols as dictated in Figures 3A and 4A were developed based on our previous study to differentiate iPSCs and hESCs into islet organoids.^{13,31} At Stage 1 (S1) (Figure 3A): cells were differentiated in RPMI 1640 (Corning Life Science) supplemented with serum-free B27 (Gibco), 50 ng/mL activin A (PeproTech), and 1 mM sodium butyrate (NaB, Sigma-Aldrich) for 24 h. The NaB was reduced into 0.5 mM from day 2 to day 4. Media at Stage 2 (S2) consisted of RPMI 1640, B27, 250 μM ascorbic acid (Vc, Sigma-Aldrich), 50 ng/mL keratinocyte growth factor (KGF, PeproTech), 50 ng/mL Noggin (PeproTech), 1 μM retinoic acid (RA, Sigma-Aldrich), 300 nM (−)-indolactam V (ILV, AdipoGen), and 100 nM LDN193189 (LDN, Sigma-Aldrich). At Stage 3 (S3), cells were cultured in DMEM/F12 (HyClone) containing B27, 1 μM RA, 200 nM LDN, 300 nM ILV, 1 μM 3,3',5-triiodo-L-thyronine sodium salt (T3, Sigma-Aldrich), 10 μM ALK5 inhibitor II (ALKi, Enzo Life Sciences), 10 $\mu\text{g}/\text{mL}$ heparin (HP, Sigma-Aldrich), and supplemented glucose to a final concentration of 20 mM. At Stage 4 (S4), the differentiation media contained RPMI 1640, B27, 1 μM T3, 10 μM ALKi, 1 mM N-acetyl cysteine (N-Cys, Sigma-Aldrich), 0.5 μM R428 (SelleckChem), 10 μM trolox (Enzo Life Sciences), 100 nM γ -secretase inhibitor XX (SiXX, Millipore), 10 μM zinc sulfate (Sigma-Aldrich), 10 mM nicotinamide (Nic, Sigma-Aldrich), 10 $\mu\text{g}/\text{mL}$ HP, and 20 mM glucose. At Stage 5 (S5) culture (Figure 4A), the medium was replaced with CMRL supplement containing 2% fetal bovine serum (ATCC), 1 μM T3, 10 μM ALKi, 0.5 μM R428, 100 nM SiXX, and 10 mM Nic for 7 days. All differentiation media were exchanged every

2 days. For aggregate culture, differentiated cells at the end of S3 were dissociated with Dispase (StemCell Technologies), followed by culturing in the S4 differentiation medium for 7 days and the S5 differentiation medium for another 7 days in 24-well ultralow attachment plates (Corning Life Science) without the presence of M or M+d.

TaqMan Quantitative Real-Time PCR. For quantitative real-time PCR (qRT-PCR), total ribonucleic acid (RNA) was extracted using an RNeasy mini kit (QIAGEN) and subjected to a CFX Connect RT-PCR system (Bio-Rad) as described previously in our work.^{32,33} Non-reversely transcribed RNA samples served as negative controls. Primers and probes used are listed in Table S1-Sn. Data were normalized to an internal gene (cyclophilin A) as a fold change relative to undifferentiated cells maintained on Matrigel substrates. Human pancreatic RNA (Clontech) and human islet RNA were used as positive controls.

Immunofluorescence Microscopy. Immunofluorescence microscopy was carried out as described in our earlier work.^{31,34} Primary and secondary antibodies used are shown in Table S2-Sn. Images were captured using a Zeiss 880 multiphoton confocal laser scanning microscope. For cryosectioning, differentiated aggregates were collected and fixed using 4% paraformaldehyde on ice for 1 h, followed by an additional incubation in 30% sucrose solution (w/v) overnight at 4 °C, after which the samples were embedded in OCT solution (Thermo Fisher Scientific) and sectioned at 7 μm thickness. The sections were then permeabilized and blocked with Foxp3/transcription factor fixation/permeabilization solution (Thermo Fisher Scientific), followed by antibody staining. The sections were counterstained with Vectashield mounting medium containing 4,6-diamidino-2-phenylindole (DAPI). Images were captured using a Zeiss 880 multiphoton laser scanning microscope. To measure immunolabeled endocrine cells (>3000 cells) under each treatment, fluorescent images of aggregates ($n = 18$ –38) were quantified by ImageJ (V1.50b) using a programmed macro. The contrast threshold was set between 80 and 255 and individual cells were separated by automatic watershed function. Cell number was counted with particle size larger than 200.

Glucose Stimulated Insulin Secretion. To measure glucose stimulated insulin secretion (GSIS), serum-free differentiation media were applied for stepwise differentiation. The 2% fetal bovine serum was replaced with 2% BSA in the differentiation medium of Stage 5 to rule out any potential interference from the serum. The hPSC-derived organoids were washed twice with PBS, followed by incubation in Krebs–Ringer buffer (KRB, Boston BioProducts) for 4 h. The organoids were separately incubated with KRB containing 2 or 20 mM d-GLUCOSE at 37 °C for 30 min. The respective supernatants were collected and subjected to a human insulin enzyme-link immunosorbent assay (ELISA) kit (Mercodia Inc.). Total DNA content from each sample was determined by a DNeasy Blood and Tissue Kit (QIAGEN) and Synergy H1 Microplate Reader (BioTek). Human islets purchased from Prodo Laboratories Inc. were used as positive controls.

Glucose-Regulated GCG Secretion. For glucose-stimulated GCG secretion (GSGS) test, the organoids cultured in S5 medium containing 10 μM H-1152 (Enzo Life Sciences) and 20 mM glucose for 7 days were washed twice with KRB containing 20 mM glucose and then incubated in 20 mM glucose containing KRB at 37 °C for 4 h. Then, the organoids were separately incubated with KRB containing 2 or 20 mM d-glucoset 37 °C for 30 min. The respective supernatants were collected and subjected to a human GCG chemiluminescent ELISA kit (Millipore). Human islets purchased from Prodo Laboratories Inc. were used as positive controls.

Statistical Analysis. Data are presented as means \pm standard deviation (SD) of at least three times of independent experiments. Statistical analysis was performed using one-way ANOVA with Tukey's post hoc test. Two-tail unpaired Student's *t*-test was performed for comparison between two groups. The difference was considered significant with *p* values < 0.05 .

RESULTS

Preparation of the dpECM. A number of methods were developed in the last two decades for preparing decellularized ECM from human and animal tissue samples. Most of these protocols require the use of detergents harsh to the preservation of valuable proteins such as growth factors and cytokines in decellularized ECM.^{35–37} Moreover, optimized protocol for pancreatic tissue in particular is lacking. To circumvent the detrimental effects of detergents, we developed three detergent-free (DF) methods and compared them against two previously reported detergent-based (DB) methods,^{38,39} as shown in Figure 1A. Although all protocols

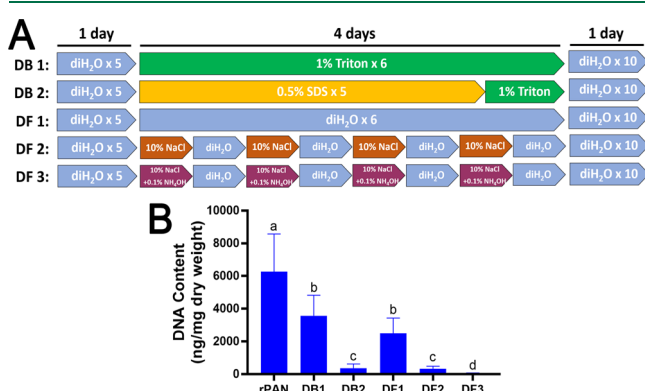


Figure 1. Optimization of decellularization procedures for pancreatic tissue. (A) Overview of a variety of decellularization strategies. Two DB and three DF methods were examined. (B) Residual DNA content of pancreatic tissue treated by different decellularization protocols. DNAs were extracted from lyophilized samples and normalized to the weight of each sample. Lyophilized rat pancreas (rPAN) without decellularization was used as a control. Data are presented as mean \pm SD ($n = 3$). Different letters (a–f) above the bars represent that the bars are significantly different from each other.

showed a reduction of cellular DNA compared to the native tissue, the differences between these individual protocols were remarkable (Figure 1B). Hypertonic saline-treated groups (Figure 1B, DF2 and DF3) showed the least residual DNA, whereas the addition of ammonium hydroxide in the saline solution (Figure 1B, DF3) further reduced DNA content to an almost undetectable level (60 ± 50 ng/mg dry weight). The results are in a similar range as found in a previous study of murine pancreas, which showed 41 ± 12 ng/mg dry weight in decellularized pancreas.³⁹

As our goal is to use dpECM as a signaling substrate for surface coating of culture plates in addition to the growth factor-reduced Matrigel, the DF3 method was chosen to prepare dpECM for further experimentation. Pancreatic tissue samples turned into a translucent white color with decreased volume after decellularization (Figure 2A,B). We performed H&E staining to show both nuclei and the ECM fiber structure (Figure 2C,D). We did not detect any intact nuclei by hematoxylin staining after decellularization; only matrix proteins were detected by eosin staining, showing a pink color in H&E staining (Figure 2D). The detection of residual DNA content in the dpECM suggested a complete removal of cells from the tissue (Figure 2E). 99% DNA in the dpECM was successfully removed from the tissue (Figure 2F). A homogeneous and translucent dpECM solution was obtained by solubilizing the dpECM in acetic acid in the presence of pepsin (Figure 2G). The ultrastructure of solubilized dpECM

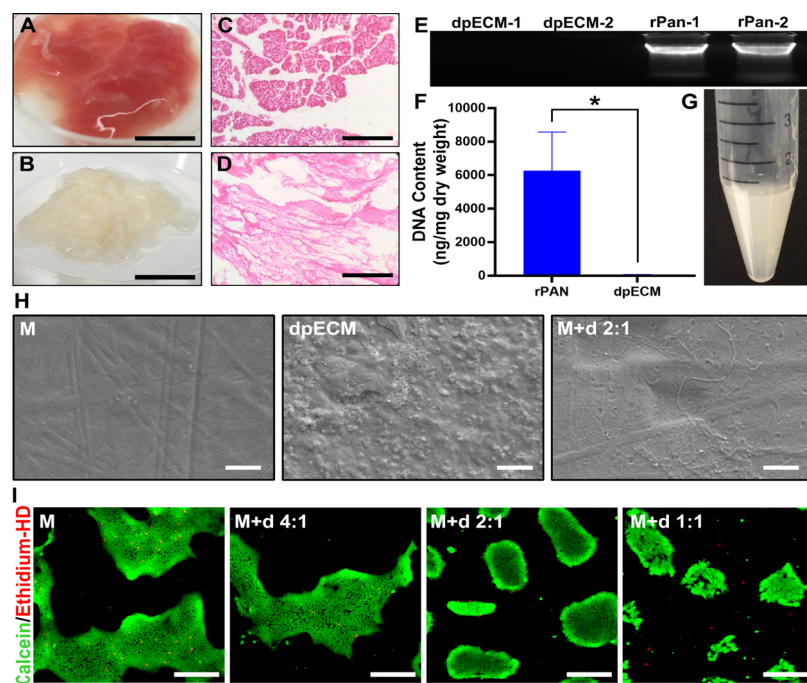


Figure 2. Preparation of dpECM substrate and its characterization. Micrographs of rat pancreatic tissues (A) before and (B) after decellularization. Scale bars, 1 cm. (C,D) H&E staining of rat pancreatic tissues (C) before and (D) after decellularization. Scale bars, 200 μ m. (E) Gel electrophoresis of DNAs extracted from two dpECM replicates. Equal amounts of native rat pancreatic tissues were served as a control (rPan). (F) DNA content (mean \pm SD) detected in dpECM as compared to that in pancreatic tissues before decellularization ($n > 3$). * $p < 0.05$. (G) Reconstituted dpECM. (H) SEM images of Matrikel (M)-, dpECM-, or mixture of Matrikel and dpECM (2:1 (w/w)) (M+d)-coated surfaces. Scale bars, 1 μ m. (I) Live/dead cell dual-color staining of iPSCs cultured on either Matrikel (M)-coated or a mixture of Matrikel and dpECM (M+d) substrate-coated plates at various ratios for 24 h after seeding. Scale bars, 200 μ m.

as a coating material was analyzed by SEM. In contrast to the smooth surface after Matrikel coating (referred to “M”), dpECM coating showed a complete deposition of grooves, ridges, and fibrillar meshwork (Figure 2H), whereas Matrikel mixed with the dpECM (referred to “M+d”) showed a uniform layer with certain fibrillar structures.

Upon the preparation of the dpECM, we interrogated whether iPSCs can attach to and proliferate on dpECM substrates. Although no iPSCs could attach to the dpECM substrates (data not shown), iPSCs attached to and proliferated on M+d mixed substrates (Figure 2I). Proteomics analysis confirmed the shortage of adhesion molecules, such as laminin and vitronectin in dpECM for hPSC attachment (Table 1). We observed that five types of laminin and some adhesion proteins exclusively exist in Matrikel, in which laminin $\alpha 1$, laminin $\alpha 4$, laminin $\alpha 5$, laminin $\beta 1$, and vitronectin were identified from all three batches of Matrikel. The adhesion molecules entailed in Matrikel enabled the iPSCs to grow on the substrates (Table 1). An increase in the concentration of the dpECM in the mixture of M+d substrates led to a considerable decrease in cell attachment and growth, which further confirms the adverse effect of the dpECM on iPSC attachment. Hence, the concentration of the dpECM in the mixture substrates needs to be carefully determined. As shown in Table 1, few glycosaminoglycans exist in the dpECM and Matrikel, which ruled out potential formation of proteoglycan complexes for binding growth factors during cell attachment.

Instructive Effects of the dpECM on Islet Development from iPSCs. Next, we intended to interrogate whether the dpECM includes signaling molecules that induce islet development during iPSC pancreatic differentiation. Thus,

Table 1. Comparison of Adhesion Molecules and Glycosaminoglycans Identified in Matrikel (M) and dpECM^a

name	identified in M with frequency	identified in dpECM with frequency
laminin $\alpha 1$	+(3/3)	+(1/3)
laminin $\alpha 2$	+(2/3)	
laminin $\alpha 3$	+(1/3)	
laminin $\alpha 4$	+(3/3)	
laminin $\alpha 5$	+(3/3)	
laminin $\beta 1$	+(3/3)	+(1/3)
laminin $\beta 2$	+(2/3)	+(1/3)
laminin $\gamma 1$	+(3/3)	+(2/3)
laminin $\gamma 3$	+(1/3)	
fibronectin	+(3/3)	+(2/3)
vitronectin	+(3/3)	
heparan sulfate	+(2/3)	
chondroitin sulfate		
dermatan sulfate		
keratan sulfate		

^a $n = 3$ for M and dpECM, respectively.

iPSCs were differentiated into pancreatic lineages following a protocol developed at our lab with some modifications (Figure 3A).^{13,40} This protocol yields in a stepwise fashion definitive endoderm (DE) (S1), posterior foregut (S2), pancreatic progenitor (S3), and hormone-expressing endocrine cells (S4). We performed immunofluorescence microscopy to ascertain the composition of the cells at the end of Stage 4. As exhibited in Figure 3, we detected all major hormone-

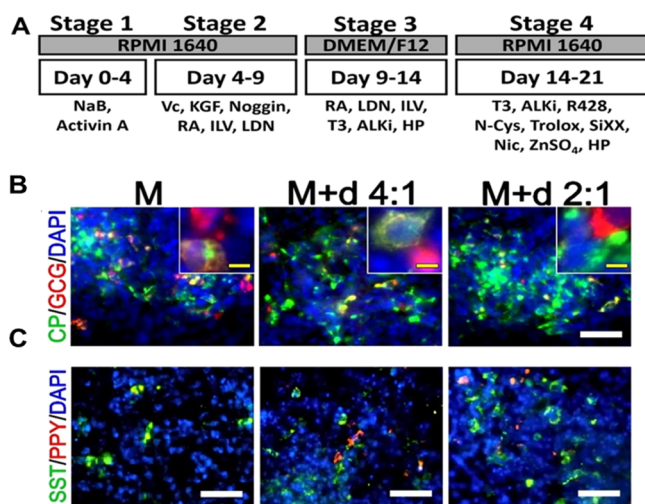


Figure 3. dpECM promotes self-assembly of islet-like architecture during iPSC pancreatic islet differentiation. (A) Four-stage and 21 day protocol for differentiating iPSCs into islet tissues. Basal media as well as key molecules used at each stage of differentiation are shown in the diagram. (B,C) Structure of iPSC-derived islet-like organoids formed in the presence of dpECM cues. iPSCs were induced for differentiation on Matrigel (M)-coated or Matrigel and dpECM (M+d) mixed substrate-coated plates at the ratio of 4:1 or 2:1 (w/w). At the end of four-stage differentiation, the cells were immunofluorescently labeled for (B) CP (green) and GCG (red) and (C) SST (green) and PPY (red). DAPI (blue) was used for counterstaining the cell nuclei. White scale bars, 50 μ m; yellow scale bars, 10 μ m.

secretory pancreatic islet cell types in the clusters, which include insulin (INS)-secreting β cells that produce C-peptide (CP), GCG-secreting α cells, SST-secreting δ cells, and pancreatic polypeptide (PPY)-secreting PP cells. Examining

the tissue architecture of these cell clusters revealed that β cells were intermingled with α , δ , and PP cells, which reassembles a characteristic tissue structure of adult human islets. In contrast, no PP cells were detected in clusters formed on the Matrigel substrates. It is worth pointing out that only few cell clusters were formed on the Matrigel substrates. It appeared that most islet cells differentiated on the M or 4:1 mixed M+d substrates were polyhormone-expressing cells, which suggest their immaturity. By contrast, islet cells generated on the 2:1 mixed M+d substrates were more monohormonal-expression cells, which suggest their maturity. These experiments evidently suggested an instructive effect of the dpECM on islet development during iPSC pancreatic differentiation. To determine whether these cell clusters are glucose responsive, we performed a GSIS assay. No glucose-responsive insulin secretion could be detected from these cell clusters upon glucose challenges (data not shown), which suggests their low degree of functionality.

dpECM Cues Recapitulate Islet Organogenesis and Morphogenesis and Promote Maturation of Islet Organoids in the Combination of Two-Dimensional and Three-Dimensional Cultures. Recent studies indicated that pancreatic endocrine cells require extra time and a three-dimensional (3D) environment to mature after pancreatic endoderm specification.^{12,13,15,41} To test whether an extended culture in a pancreatic preferential medium under 3D conditions could help mature cell clusters into islet organoids, we designed a five-stage differentiation protocol (Figure 4A). We collected cell clusters at the end of Stage 3 and transferred them to ultralow attachment culture plates to mature them in a 3D suspension culture without the presence of M or M+d for another 2 weeks. At the end of the five-stage differentiation, the expression of key endocrine marker genes in iPSC-derived

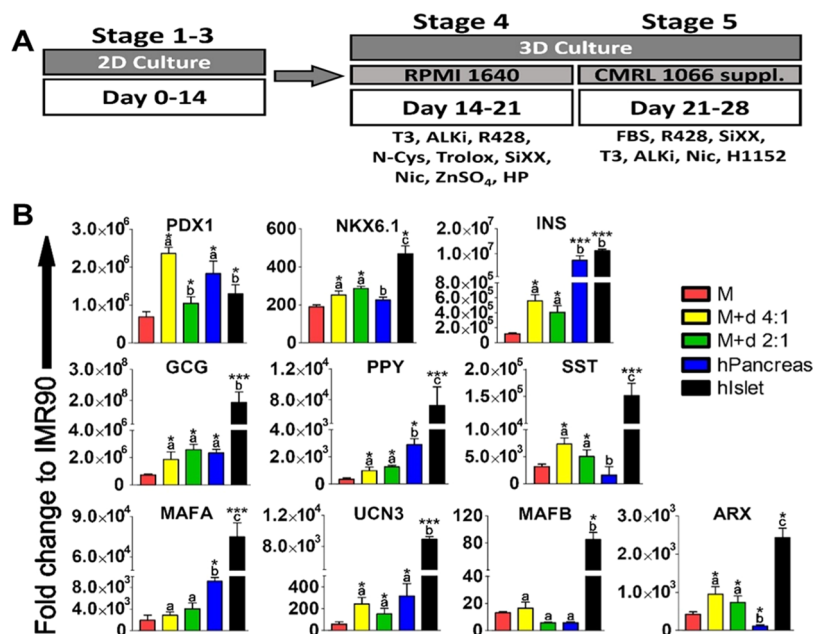


Figure 4. Enhancement of islet-like organoid development in the presence of dpECM substrates. (A) Scheme of five-stage islet development. (B) iPSCs were induced for differentiation on Matrigel (M)-coated or Matrigel and dpECM (M+d) mixed substrate-coated plates at ratio of 4:1 or 2:1 (w/w). At the end of five-stage differentiation, the expression levels of endocrine marker genes in the organoids were quantified by qRT-PCR and normalized to undifferentiated IMR90 cells. Results are from three independent differentiation experiments ($n = 3$) and shown as mean \pm SD. * $p < 0.05$ and *** $p < 0.001$ compared to the M group. Different letters (a or b) above the bars represent that the bars are significantly different from each other. Human pancreatic RNA (hPancreas) and human islet RNA (hIslet) were used as positive controls.

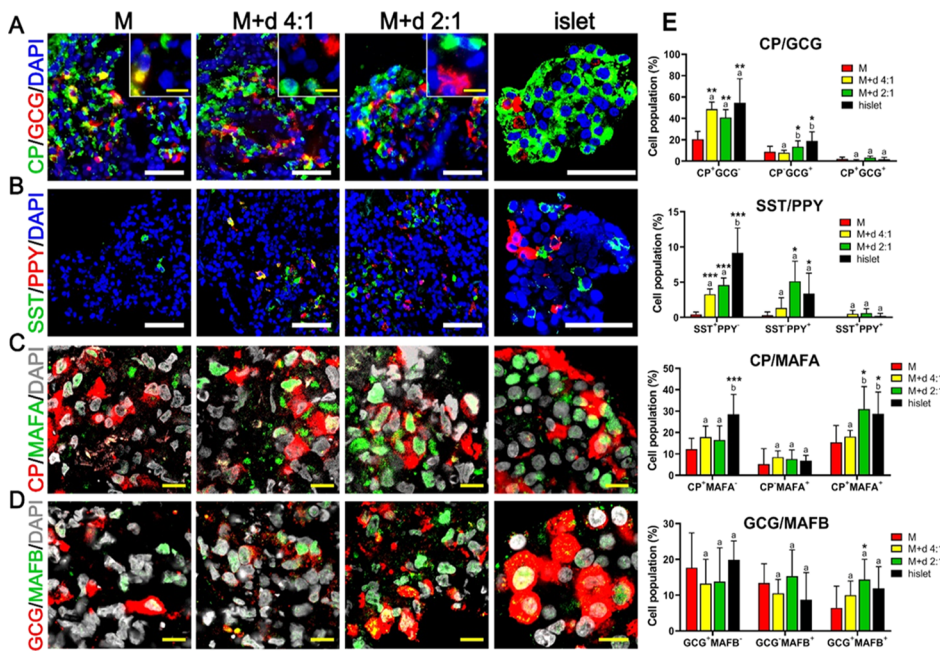


Figure 5. Enhancement of organogenesis and morphogenesis of iPSC-derived islet organoids in extended 3D cultures. iPSCs were induced to differentiate to endocrine tissues on Matrigel (M)-coated or Matrigel and dpECM (M+d) mixed substrate-coated plates at the indicated ratios of Matrigel to dpECM, following a five-stage differentiation protocol. The samples were immunofluorescently labeled for (A) CP (green) and GCG (red); (B) SST (green) and PPY (red); (C) MAFA (green) and CP (red); and (D) MAFB (green) and GCG (red). Cells were counterstained with DAPI (blue). (E) Characterization of the architecture of iPSC-derived islet organoids. Images were quantified to estimate approximate populations of each cell subtype using ImageJ ($n = 18-38$). Results are shown as mean \pm SD. * $p < 0.05$; ** $p < 0.01$; and *** $p < 0.001$ compared to the M group. Groups with different letters represent significant differences. Human islets (islet) were used as a positive control. White scale bars, 50 μ m; yellow scale bars, 10 μ m.

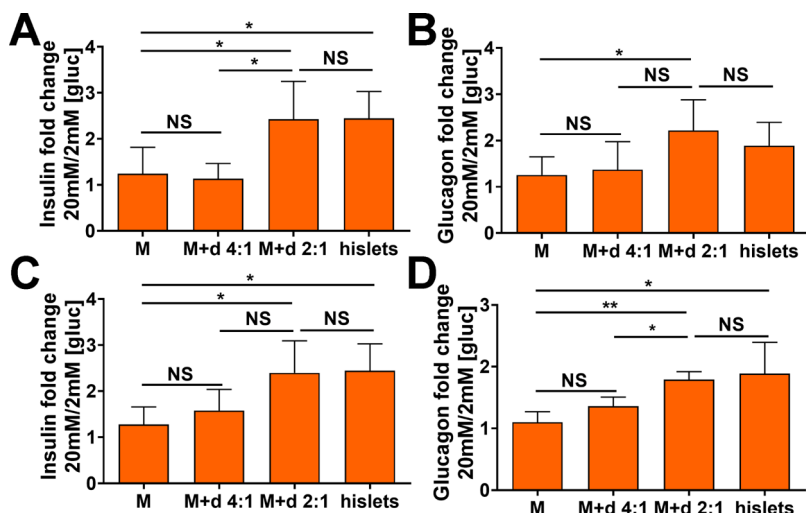


Figure 6. Glucose-responsive secretions of insulin and GCG from hPSC-derived islet organoids at the end of five-stage stepwise differentiation. (A,B) iPSC line IMR90 cells- and (C,D) hESC line H9- derived organoids were challenged with low (2 mM) and high (20 mM) glucose. (A,C) Glucose-regulated insulin secretion was assessed by fold change calculated as the ratio of insulin secreted in high glucose conditions to that in low glucose conditions. IMR90 (A) ($n = 3$) and H9 (C) ($n = 3$). (B,D) Glucose-regulated GCG secretion was assessed by fold change calculated as the ratio of GCG secreted in low glucose conditions to that in high glucose conditions. IMR90 (B) ($n = 6$) and H9 (D) ($n = 3$). Human donor islets (islets, $n = 4$) were used as a control. Data shown are means \pm SD. * $p < 0.05$; ** $p < 0.01$; NS: not significant.

cells generated on the M+d substrates showed increased expressions of PDX-1, NKX6.1, INS, GCG, PPY, SST, urocortin 3 (UCN3), and aristaless-related homeobox (ARX) compared to the M group (Figure 4B). Increasing the dpECM concentration above 2:1 did not appear to enhance the iPSC pancreatic differentiation (data not shown). It is noteworthy that although the expression of endocrine marker genes

increased significantly in M+d groups, they did not show comparable levels to those in human pancreas or islets except for PDX-1.

To examine whether the islet organogenesis and morphogenesis were elevated during the extended 3D cultures, we determined morphology and tissue architecture of the organoids through immunofluorescence microscopy. The

Table 2. Approaches for the Generation of Human Islets from Pluripotent Stem Cells

reference	stepwise differentiation timeline (days)	strategy	cell line	GSIS (fold change)	GSGS (fold change)	δ cells	PP cells
this work	5-stage (28)	2D for 18 days; 3D suspension for 10 days	IMR90, H9	~2.8	2	detected	detected
(Kim et al., 2018) ³⁷	5-stage (26)	pillar/pore polystyrene nanopattern; suspension culture at stage 5	H1	N/A	N/A	N/A	N/A
(Wang et al., 2017) ¹³	4-stage (22–23)	3D cell-laden scaffold culture	H9	~3.5	N/A	detected	detected
(Kim et al., 2016) ²⁷	4-stage (17)	1-day suspension on last day of differentiation	H1, CHA15	2.5	N/A	N/A	not detected
(Shaer et al., 2016) ⁵⁸	4-stage (31)	2D with microRNA-7 transfection	RSCB0082	~1.40	N/A	N/A	N/A
(Shaer et al., 2014) ²⁴	4-stage (31)	2D	RSCB0082	N/A	N/A	N/A	N/A
(Rezania et al., 2014) ¹⁶	7-stage (30–40)	2D at stage 1–4; 3D suspension at stage 5–7	H1, homemade iPSC	1.7	N/A	detected	not detected
(Pagliuca et al., 2014) ¹²	6-stage (30–37)	suspension culture in spinner flasks	HUES8, homemade iPSC	~3.0	N/A	N/A	N/A
(Tateishi et al., 2008) ²³	4-stage (29)	2D	H9, homemade iPSC	N/A	N/A	N/A	N/A
(Jiang et al., 2007) ²²	4-stage (36)	2D	H1, H7, H9	3.3	N/A	N/A	N/A

analysis of cellularity of the organoids formed on the M+d substrates demonstrated a tissue architecture similar to human islets (Figure 5). It should be pointed out that there are no reliable markers that can be used to separate islet organoids from other cell aggregates through flow cytometry. In addition, the efficiency of the generation of islet organoids remains low. Hence, flow cytometry failed to estimate the islet cell subpopulations from the entire population containing many non-islet cells. In order to characterize morphogenesis of these organoids to determine heterogeneity and estimate the organoids' cell composition, we performed cryo-sectioning, immunostaining, and fluorescence microscopy, followed by calculating the percentage of each type of endocrine cells in the organoids using ImageJ, as reported previously.⁴² The images ($n = 18–38$) of each subtype of islet cells were quantified. A significant increase of CP⁺/GCG[−] and CP[−]/GCG⁺ monoclonal cells were found in the M+d groups with distributions of those cells comparable to that found in human islets (Figure 5A). In addition, the organoids formed on the 2:1 mixed M+d substrates yielded more SST⁺ and PPY⁺ cells during the extended cultures as compared to the cells in the Matrigel group (Figure 5B).

MAFA and MAFB are the two transcription factors in adult β - and α -cells, respectively. They are critical for islet maturation.^{11,43–45} Multiplex staining of CP, GCG, MAFA, and MAFB of the organoids revealed a large amount of MAFA and MAFB in the nuclei of islet cells formed on the M+d substrates (Figure 5C,D). As shown in Figure 5E, the CP⁺/MAFA⁺ and GCG⁺/MAFB⁺ cells in the M+d 4:1 group increased slightly as compared to those in the M group, although not significantly. We speculated that the concentration of instructive factors in the M+d 4:1 was not high enough to induce islet development. By increasing the dosage of dpECM in the mixture, we observed a significant increase in CP⁺/MAFA⁺ and GCG⁺/MAFB⁺ cells in the M+d 2:1 group. Together, we demonstrated that the dpECM promotes islet organogenesis and morphogenesis during iPSC pancreatic differentiation.

Further investigation by the GSIS assay confirmed that the organoids cultured in two-dimensional (2D) conditions did not show glucose-responsiveness (data not shown). In

contrast, insulin secretion in response to glucose concentrations was detected from 3D cultured organoids (Figure 6A). In cells from the M+d 2:1 group, there was approximately 2.4-fold more insulin secretion in response to glucose level changes from low (2 mM) to high (20 mM). This fold change of insulin release under glucose challenge was similar to that in donor islets (Figure 6A). It appeared that cells in M and M+d groups did not show glucose responsiveness, which is consistent with the results obtained in Figure 5.

Islet Organoids Matured in Extended Three-Dimensional Cultures Secrete Glucose-Regulated GCG. To evaluate further the potential of the organoids in hormonal glycemic control and nutrient homeostasis, we assessed whether the organoids secrete GCG in response to glucose levels. We observed that glucose-regulated GCG secretion from the organoids cultured in the M+d 2:1 group improved significantly as compared to that in the control and M+d 4:1 groups ($p < 0.05$) (Figure 6B). The GCG secretion was sugar-level responsive with similar sensitivity to that detected in human donor islets. The experimental results indicated a glucose-responsive GCG secretion from α cells. Taken together, for the first time, we demonstrated a successful generation of iPSC-derived physiologically functional islet organoids with glucoregulatory production of both insulin and GCG.

Having characterized the unique role the dpECM played in human iPSC islet development, we next investigated whether the instructive effect of the dpECM on islet development is reproducible to hESCs as well. We performed hESC pancreatic differentiation after spiking with the dpECM. hESC H9 line was used for these experiments. As shown in Figure 6C,D, hESC-derived islet organoids also demonstrated glucose-responsive insulin and GCG secretions, similar to that observed in iPSC-derived islet organoids.

DISCUSSION

Organoids were recently defined by the American Society for Cell Biology as generated using renewable tissue sources, such as human stem cells, under controlled cultured conditions. They self-organize to 3D structures, recapitulate development and tissue organization, and/or incorporate multiple aspects of

the cellular complexity of the modeled tissue.⁴⁶ In this study, we discovered that the tissue-specific dpECM could induce islet organogenesis and morphogenesis during hPSC islet differentiation. We corroborated that the dpECM triggers the self-assembly of organoids during hPSC differentiation toward islet tissues. These organoids secreted both insulin and GCG in response to glucose levels (Figure 6). Although the absolute amount of insulin secreted from iPSC-derived organoids was very low compared to human donor islets, GCG production from the organoids is comparable to that secreted from human islets (data not shown), suggesting that they are capable of physiological hormone secretion and a degree of maturation. The organoids are composed of pancreatic endocrine cells with similar proportions found in human islets.⁴⁷ As summarized in Table 2, to our best knowledge, current approaches for the generation of human islet organoids emphasize only on insulin secretion, whereas the analysis of functional α cells is absent (Table 2). Hence, our findings of glucose-responsive insulin and GCG production from hPSC-derived islet organoids are substantial and promising. We also showed that the spiking of hPSCs with the dpECM elevates the expression of key pancreatic transcription factors that include PDX-1, NKX6.1, UCN3, ARX, and hormones in the organoids. The iPSC-derived islet organoids showed multiple types of endocrine cells with similar proportions to adult islets, which consist of four major islet cell types, that is, α , β , δ , and PP cells that harbor geometrically unique reciprocal cell–cell interactions. Importantly, we achieved a similar glucose-responsive hormone-release behavior in organoids developed from both iPSCs and hESCs, although considerable variations in maturation have been observed when different hPSC lines are used for organoid development.⁴⁸ Consequently, our results suggest the robustness of dpECM cues to islet development from hPSCs.

Another interesting observation through this study is the importance of dpECM preparation. By comparing a variety of decellularization methods, we showed that alternating between hyper- and hypotonic solutions is the most effective approach in removing cellular components. Compared to previously reported decellularization methods for pancreatic tissue, which require the use of detergents such as 1% Triton X-100³⁸ or 0.5% SDS combined with 1% Triton X-100,³⁹ the dpECM generated using the method developed in this study contained the least residual DNA (Figure 1B). Our data showed that the dpECM contains less than 1% of DNA, and that no large DNA fragments can be detected after decellularization. These properties satisfy the criteria of an ideal nonimmunogenic acellular biomaterial described previously.⁴⁹ In addition to the effectiveness of removing cellular contents, the reagents used are easily rinsed off when compared to flushing detergents out of decellularized tissues. Although the dpECM was found to be nontoxic to hPSCs, a remarkable decrease of cellular adhesion to the dpECM substrates was observed (Figure 2I). In our recent study, we found that very limited cellular adhesion molecules in the dpECM were detected compared to those in Matrigel through mass spectrometer analysis.³¹ Adhesion molecules essential to hPSC attachment, such as laminin, fibronectin, and vitronectin, were significantly insufficient in the dpECM for hPSC attachment (Table 1).^{31,50} Matrigel is a prevailing ECM substrate for hPSC cultures. It is an extract from mouse sarcoma-derived basement membrane rich in laminin, collagen IV, and heparan sulfate proteoglycans.⁵¹ Extensive evidence has been documented about the supportive

role of Matrigel in stem cell survival, attachment, and proliferation.⁵² However, Matrigel lacks of tissue specificity that may impair tissue development from stem cells. Consequently, the mixture of the dpECM with Matrigel helps cells to attach, proliferate, differentiate, and assemble into islet organoids.

Notably, the dpECM generated in this study was fabricated from the pancreas, including both exocrine and endocrine tissues. It was reported that the compositions of exocrine and endocrine ECM are very similar.⁵³ We hypothesized that some key molecules in a decellularized pancreas would provide signaling for iPSC pancreatic islet development due to the fact that the pancreatic organ provides unique microenvironments for maintaining islet functions. Another study suggested that pancreatic ECM supports the survival and functionality of islets in cultures.⁵⁴ The finding of spontaneous endodermal lineage specification of embryoid bodies in a decellularized pancreas further supports our hypothesis and observation.⁵⁵ These signaling molecules in the dpECM could be ECM proteins or signaling proteins secreted from pancreatic cells. We have reported that type V collagen identified in the dpECM fabricated from animal pancreas is one of the signaling molecules promoting islet tissue development from iPSCs.³¹ This finding is consistent with our study that the dpECM is beneficial and crucial for generating functional endocrine lineage.

To mature islet organoids, we switched the hPSC islet development environment from 2D to 3D at a late stage of the differentiation. We reaggregated cells in a suspension culture for the last two stages of development. No dpECM was added to the cell culture medium. Interestingly, the omission of the dpECM in the late stages did not nullify the enhanced islet lineage progression, which indicates the critical role of the cell–dpECM interaction at the early stage of islet development. This is consistent with the previous finding that early pancreas specification stage is decisive for the formation of diverse endocrine islet cell types.^{14,56} Compared with 2D culture, the insulin secretory function of the organoids elevates significantly after 3D culture. There was approximately three-fold more insulin secreted from the 3D cultured organoids than that from 2D cultures (data not shown). These results recapitulate the previous finding that direct 3D contact is fundamentally important to the coordination of insulin secretion in β -cells.⁴⁸ Recellularizing the decellularized tissue slices with progenitor cells could be another approach to produce mature pancreatic islet cells. However, scaling this differentiation approach would be very challenging. It requires a tremendous amount of islet cells for treating one patient. Our goal is to develop a robust and scalable islet organoid manufacturing process. To this end, in this study we examined the feasibility of generating mature islet organoids using a suspension culture, which is a scalable cell culture process.

Although the mechanisms that underlie the hPSC–dpECM interaction during islet development remain elusive, we speculate that there are some tissue-specific cues presented by the dpECM to hPSCs, which lead to the induction of intrinsic pathways that direct cell differentiation toward islet organogenesis. Further studies will require the identification of these factors in order to develop a defined islet development medium to generate clinical grade islets for clinical applications. It should be pointed out that much work is needed to further increase the organoids' capability of glucose-responsive insulin and GCG secretion.

Taken together, this study highlights the instructive effect of the dpECM on islet organogenesis from hPSCs. The tissue-specific cues presented by the dpECM assemble a complex microenvironment that is critical to cell fate specification in early stage of hPSC pancreatic differentiation. These findings provide a foundation for future investigations into essential outside-in signals to produce clinically relevant pancreatic tissues. Further studies are required to determine the signaling molecules that induce organogenesis.

CONCLUSIONS

Tissue matrix substrates prepared by a DF method show removal of almost all animal cells from the pancreatic tissue. The dpECM substrates augment islet organogenesis and morphogenesis from differentiation of hPSCs. The stem cell-derived islet organoids secrete both glucose-responsive insulin and GCG, two major hormones that maintain glucose homeostasis in the blood. They consist of all major pancreatic endocrine cell types under the tissue cues of decellularized ECM substrates.

ASSOCIATED CONTENT

Supporting Information

The Supporting Information is available free of charge at <https://pubs.acs.org/doi/10.1021/acsbiomaterials.0c00088>.

List of primers and probes used in TaqMan qRT-PCR analysis and a list of antibodies used in immunofluorescence staining ([PDF](#))

AUTHOR INFORMATION

Corresponding Author

Sha Jin — Department of Biomedical Engineering and Center of Biomanufacturing for Regenerative Medicine, Binghamton University, State University of New York (SUNY), Binghamton, New York 13902, United States;  orcid.org/0000-0002-8033-8110; Phone: 607-777-5718; Email: sjin@binghamton.edu; Fax: 607-777-5780

Authors

Huanjing Bi — Department of Biomedical Engineering, Binghamton University, State University of New York (SUNY), Binghamton, New York 13902, United States

Soujanya S. Karanth — Department of Biomedical Engineering, Binghamton University, State University of New York (SUNY), Binghamton, New York 13902, United States

Kaiming Ye — Department of Biomedical Engineering and Center of Biomanufacturing for Regenerative Medicine, Binghamton University, State University of New York (SUNY), Binghamton, New York 13902, United States;  orcid.org/0000-0001-7736-9875

Roland Stein — Department of Molecular Physiology and Biophysics, Vanderbilt University, Nashville, Tennessee 37232, United States

Complete contact information is available at: <https://pubs.acs.org/10.1021/acsbiomaterials.0c00088>

Author Contributions

H.B., S.J., and K.Y. conceived and designed the experiments. H.B. and S.S.K. carried out the experiments. H.B., S.S.K., S.J., K.Y., and R.S. contributed to data analysis, interpretation, and discussion. H.B. wrote the manuscript. S.J., R.S., and K.Y.

revised the manuscript. All authors read and approved the final manuscript.

Notes

The authors declare no competing financial interest.

ACKNOWLEDGMENTS

This research was partially supported by National Science Foundation CBET1445387, 1531944, and 1928855, and State of New York Health Now Network of Excellence. The authors thank Kimberly Kal-Downs, Theresa Kolb, Cathy Wilding, and Robert Snyder from the Animal Facility at Binghamton University for providing rat pancreata. The authors thank Katherine Karlson for editorial review of this manuscript.

ABBREVIATIONS

ALK5, ALK5 inhibitor II; ARX, aristaless-related homeobox; CP, C-peptide; dpECM, decellularized pancreatic extracellular matrix; DE, definitive endoderm; DB, detergent-based; ELISA, enzyme-link immunosorbent assay; GCG, glucagon; GSIS, glucose stimulated insulin secretion; GSGS, glucose-stimulated glucagon secretion; ESCs, human embryonic stem cells; HP, heparin; ILV, indolactam V; iPSCs, induced pluripotent stem cells; INS, insulin; KGF, keratinocyte growth factor; KRB, Krebs–Ringer buffer; LDN, LDN193189; N-Cys, N-acetyl cysteine; PP cells, pancreatic polypeptide cells; PPY, pancreatic polypeptide; NaB, sodium butyrate; Nic, nicotinamide; qRT-PCR, quantitative real-time PCR; RA, retinoic acid; SDS, sodium dodecyl sulfate; SiXX, γ -secretase inhibitor XX; SST, somatostatin; T1D, type I diabetes; T2D, type II diabetes; T3, 3,3',5-triiodo-L-thyronine sodium salt; UCN3, urocortin 3; Vc, ascorbic acid; 2D, two-dimensional; 3D, three-dimensional

REFERENCES

- (1) Brissova, M.; Haliyur, R.; Saunders, D.; Shrestha, S.; Dai, C.; Blodgett, D. M.; Bottino, R.; Campbell-Thompson, M.; Aramandla, R.; Poffenberger, G.; Lindner, J.; Pan, F. C.; von Herrath, M. G.; Greiner, D. L.; Shultz, L. D.; Sanyoura, M.; Philipson, L. H.; Atkinson, M.; Harlan, D. M.; Levy, S. E.; Prasad, N.; Stein, R.; Powers, A. C. alpha Cell Function and Gene Expression Are Compromised in Type 1 Diabetes. *Cell Rep.* **2018**, *22*, 2667–2676.
- (2) Yosten, G. L. C. Alpha cell dysfunction in type 1 diabetes. *Peptides* **2018**, *100*, 54–60.
- (3) Sloop, K. W.; Michael, M. D.; Moyers, J. S. Glucagon as a target for the treatment of Type 2 diabetes. *Expert Opin. Ther. Targets* **2005**, *9*, 593–600.
- (4) Moon, J. S.; Won, K. C. Pancreatic alpha-Cell Dysfunction in Type 2 Diabetes: Old Kids on the Block. *Diabetes Metabol J.* **2015**, *39*, 1–9.
- (5) Burcelin, R.; Knauf, C.; Cani, P. D. Pancreatic alpha-cell dysfunction in diabetes. *Diabetes Metab.* **2008**, *34*, S49–S55.
- (6) Halban, P. A. Cellular sources of new pancreatic beta cells and therapeutic implications for regenerative medicine. *Nat. Cell Biol.* **2004**, *6*, 1021–1025.
- (7) Rorsman, P.; Braun, M. Regulation of insulin secretion in human pancreatic islets. *Annu. Rev. Physiol.* **2013**, *75*, 155–179.
- (8) Ishihara, H.; Maechler, P.; Gjinovci, A.; Herrera, P.-L.; Wollheim, C. B. Islet beta-cell secretion determines glucagon release from neighbouring alpha-cells. *Nat. Cell Biol.* **2003**, *5*, 330–335.
- (9) Braun, M.; Ramracheya, R.; Amisten, S.; Bengtsson, M.; Moritoh, Y.; Zhang, Q.; Johnson, P. R.; Rorsman, P. Somatostatin release, electrical activity, membrane currents and exocytosis in human pancreatic delta cells. *Diabetologia* **2009**, *52*, 1566–1578.
- (10) Batterham, R. L.; Le Roux, C. W.; Cohen, M. A.; Park, A. J.; Ellis, S. M.; Patterson, M.; Frost, G. S.; Ghatei, M. A.; Bloom, S. R.

Pancreatic polypeptide reduces appetite and food intake in humans. *J. Clin. Endocrinol. Metab.* **2003**, *88*, 3989–3992.

(11) Shapiro, A. M. J.; Lakey, J. R. T.; Ryan, E. A.; Korbutt, G. S.; Toth, E.; Warnock, G. L.; Kneteman, N. M.; Rajotte, R. V. Islet transplantation in seven patients with type 1 diabetes mellitus using a glucocorticoid-free immunosuppressive regimen. *N. Engl. J. Med.* **2000**, *343*, 230–238.

(12) Pagliuca, F. W.; Millman, J. R.; Gürler, M.; Segel, M.; Van Dervort, A.; Ryu, J. H.; Peterson, Q. P.; Greiner, D.; Melton, D. A. Generation of functional human pancreatic beta cells in vitro. *Cell* **2014**, *159*, 428–439.

(13) Wang, W.; Jin, S.; Ye, K. Development of Islet Organoids from H9 Human Embryonic Stem Cells in Biomimetic 3D Scaffolds. *Stem Cells Dev.* **2017**, *26*, 394–404.

(14) Russ, H. A.; Parent, A. V.; Ringler, J. J.; Hennings, T. G.; Nair, G. G.; Shveygert, M.; Guo, T.; Puri, S.; Haataja, L.; Cirulli, V.; Blelloch, R.; Szot, G. L.; Arvan, P.; Hebrok, M. Controlled induction of human pancreatic progenitors produces functional beta-like cells in vitro. *EMBO J.* **2015**, *34*, 1759–1772.

(15) Takeuchi, H.; Nakatsuji, N.; Suemori, H. Endodermal differentiation of human pluripotent stem cells to insulin-producing cells in 3D culture. *Sci. Rep.* **2014**, *4*, 4488.

(16) Rezania, A.; Bruin, J. E.; Arora, P.; Rubin, A.; Batushansky, I.; Asadi, A.; O'Dwyer, S.; Quiskamp, N.; Mojibian, M.; Albrecht, T.; Yang, Y. H. C.; Johnson, J. D.; Kieffer, T. J. Reversal of diabetes with insulin-producing cells derived in vitro from human pluripotent stem cells. *Nat. Biotechnol.* **2014**, *32*, 1121–1133.

(17) Rajaei, B.; Shamsara, M.; Amirabad, L. M.; Massumi, M.; Sanati, M. H. Pancreatic Endoderm-Derived from Diabetic Patient-Specific Induced Pluripotent Stem Cell Generates Glucose-Responsive Insulin-Secreting Cells. *J. Cell. Physiol.* **2017**, *232*, 2616.

(18) D'Amour, K. A.; Bang, A. G.; Eliazer, S.; Kelly, O. G.; Agulnick, A. D.; Smart, N. G.; Moorman, M. A.; Kroon, E.; Carpenter, M. K.; Baetge, E. E. Production of pancreatic hormone-expressing endocrine cells from human embryonic stem cells. *Nat. Biotechnol.* **2006**, *24*, 1392–1401.

(19) Rezania, A.; Bruin, J. E.; Xu, J.; Narayan, K.; Fox, J. K.; O'Neil, J. J.; Kieffer, T. J. Enrichment of human embryonic stem cell-derived NKX6.1-expressing pancreatic progenitor cells accelerates the maturation of insulin-secreting cells in vivo. *Stem Cells* **2013**, *31*, 2432–2442.

(20) Jiang, W.; Shi, Y.; Zhao, D.; Chen, S.; Yong, J.; Zhang, J.; Qing, T.; Sun, X.; Zhang, P.; Ding, M.; Li, D.; Deng, H. In vitro derivation of functional insulin-producing cells from human embryonic stem cells. *Cell Res.* **2007**, *17*, 333–344.

(21) Zhu, S.; Russ, H. A.; Wang, X.; Zhang, M.; Ma, T.; Xu, T.; Tang, S.; Hebrok, M.; Ding, S. Human pancreatic beta-like cells converted from fibroblasts. *Nat. Commun.* **2016**, *7*, 10080.

(22) Jiang, J.; Au, M.; Lu, K.; Eshpeter, A.; Korbutt, G.; Fisk, G.; Majumdar, A. S. Generation of insulin-producing islet-like clusters from human embryonic stem cells. *Stem Cells* **2007**, *25*, 1940–1953.

(23) Tateishi, K.; He, J.; Taranova, O.; Liang, G.; D'Alessio, A. C.; Zhang, Y. Generation of insulin-secreting islet-like clusters from human skin fibroblasts. *J. Biol. Chem.* **2008**, *283*, 31601–31607.

(24) Shaer, A.; Azarpira, N.; Karimi, M. H. Differentiation of human induced pluripotent stem cells into insulin-like cell clusters with miR-186 and miR-375 by using chemical transfection. *Appl. Biochem. Biotechnol.* **2014**, *174*, 242–258.

(25) Shim, J.-H.; Kim, J.; Han, J.; An, S. Y.; Jang, Y. J.; Son, J.; Woo, D.-H.; Kim, S.-K.; Kim, J.-H. Pancreatic Islet-Like Three-Dimensional Aggregates Derived From Human Embryonic Stem Cells Ameliorate Hyperglycemia in Streptozotocin-Induced Diabetic Mice. *Cell Transplant.* **2015**, *24*, 2155–2168.

(26) Gupta, S. K.; Wesolowska-Andersen, A.; Ringgaard, A. K.; Jaiswal, H.; Song, L.; Hastoy, B.; Ingvorsen, C.; Taheri-Ghahfarokhi, A.; Magnusson, B.; Maresca, M.; Jensen, R. R.; Beer, N. L.; Fels, J. J.; Grunnet, L. G.; Thomas, M. K.; Gloyn, A. L.; Hicks, R.; McCarthy, M. I.; Hansson, M.; Honoré, C. NKX6.1 induced pluripotent stem cell reporter lines for isolation and analysis of functionally relevant neuronal and pancreas populations. *Stem Cell Res.* **2018**, *29*, 220–231.

(27) Kim, Y.; Kim, H.; Ko, U. H.; Oh, Y.; Lim, A.; Sohn, J.-W.; Shin, J. H.; Kim, H.; Han, Y.-M. Islet-like organoids derived from human pluripotent stem cells efficiently function in the glucose responsiveness in vitro and in vivo. *Sci. Rep.* **2016**, *6*, 35145.

(28) Konagaya, S.; Iwata, H. Reproducible preparation of spheroids of pancreatic hormone positive cells from human iPS cells: An in vitro study. *Biochim. Biophys. Acta, Gen. Subj.* **2016**, *1860*, 2008–2016.

(29) Chao, K. C.; Chao, K. F.; Fu, Y. S.; Liu, S. H. Islet-like clusters derived from mesenchymal stem cells in Wharton's Jelly of the human umbilical cord for transplantation to control type 1 diabetes. *PLoS One* **2008**, *3*, No. e1451.

(30) Kobayashi, T.; Yamaguchi, T.; Hamanaka, S.; Kato-Itoh, M.; Yamazaki, Y.; Ibata, M.; Sato, H.; Lee, Y.-S.; Usui, J.-i.; Knisely, A. S.; Hirabayashi, M.; Nakauchi, H. Generation of rat pancreas in mouse by interspecific blastocyst injection of pluripotent stem cells. *Cell* **2010**, *142*, 787–799.

(31) Bi, H.; Ye, K.; Jin, S. Proteomic analysis of decellularized pancreatic matrix identifies collagen V as a critical regulator for islet organogenesis from human pluripotent stem cells. *Biomaterials* **2020**, *233*, 119673.

(32) Jin, S.; Yao, H.; Weber, J. L.; Melkoumian, Z. K.; Ye, K. A synthetic, xeno-free peptide surface for expansion and directed differentiation of human induced pluripotent stem cells. *PLoS One* **2012**, *7*, No. e50880.

(33) Jin, S.; Yao, H.; Krisanarungson, P.; Haukas, A.; Ye, K. Porous membrane substrates offer better niches to enhance the Wnt signaling and promote human embryonic stem cell growth and differentiation. *Tissue Eng., Part A* **2012**, *18*, 1419–1430.

(34) Wen, Y.; Jin, S. Production of neural stem cells from human pluripotent stem cells. *J. Biotechnol.* **2014**, *188*, 122–129.

(35) Faulk, D. M.; Carruthers, C. A.; Warner, H. J.; Kramer, C. R.; Reing, J. E.; Zhang, L.; D'Amore, A.; Badylak, S. F. The effect of detergents on the basement membrane complex of a biologic scaffold material. *Acta Biomater.* **2014**, *10*, 183–193.

(36) Poornajad, N.; Schaumann, L. B.; Buckmiller, E. M.; Momtahan, N.; Gassman, J. R.; Ma, H. H.; Roeder, B. L.; Reynolds, P. R.; Cook, A. D. The impact of decellularization agents on renal tissue extracellular matrix. *J. Biomater. Appl.* **2016**, *31*, 521–533.

(37) Bi, H.; Ming, L.; Cheng, R.; Luo, H.; Zhang, Y.; Jin, Y. Liver extracellular matrix promotes BM-MSCs hepatic differentiation and reversal of liver fibrosis through activation of integrin pathway. *J. Regen. Med. Tissue Eng.* **2016**, *11*, 2685.

(38) Mirmalek-Sani, S.-H.; Orlando, G.; McQuilling, J. P.; Pareda, R.; Mack, D. L.; Salvatori, M.; Farney, A. C.; Stratta, R. J.; Atala, A.; Opara, E. C.; Soker, S. Porcine pancreas extracellular matrix as a platform for endocrine pancreas bioengineering. *Biomaterials* **2013**, *34*, 5488–5495.

(39) Goh, S.-K.; Bertera, S.; Olsen, P.; Candiello, J. E.; Halftier, W.; Uechi, G.; Balasubramani, M.; Johnson, S. A.; Sicari, B. M.; Kollar, E.; Badylak, S. F.; Banerjee, I. Perfusion-decellularized pancreas as a natural 3D scaffold for pancreatic tissue and whole organ engineering. *Biomaterials* **2013**, *34*, 6760–6772.

(40) Wang, X.; Ye, K. Three-dimensional differentiation of embryonic stem cells into islet-like insulin-producing clusters. *Tissue Eng., Part A* **2009**, *15*, 1941–1952.

(41) Vegas, A. J.; Veiseh, O.; Gürler, M.; Millman, J. R.; Pagliuca, F. W.; Bader, A. R.; Doloff, J. C.; Li, J.; Chen, M.; Olejnik, K.; Tam, H. H.; Jhunjhunwala, S.; Langan, E.; Aresta-Dasilva, S.; Gandham, S.; McGarrigle, J. J.; Bochenek, M. A.; Hollister-Lock, J.; Oberholzer, J.; Greiner, D. L.; Weir, G. C.; Melton, D. A.; Langer, R.; Anderson, D. G. Long-term glycemic control using polymer-encapsulated human stem cell-derived beta cells in immune-competent mice. *Nat. Med.* **2016**, *22*, 306–311.

(42) Youngblood, R. L.; Sampson, J. P.; Lebioda, K. R.; Shea, L. D. Microporous scaffolds support assembly and differentiation of

pancreatic progenitors into beta-cell clusters. *Acta Biomater.* **2019**, *96*, 111.

(43) Maffi, P.; Secchi, A. The Burden of Diabetes: Emerging Data. *Dev. Ophthalmol.* **2017**, *60*, 1–5.

(44) Matsuoka, T.-a.; Artner, I.; Henderson, E.; Means, A.; Sander, M.; Stein, R. The MafA transcription factor appears to be responsible for tissue-specific expression of insulin. *Proc. Natl. Acad. Sci. U. S. A.* **2004**, *101*, 2930–2933.

(45) Nostro, M. C.; Sarangi, F.; Yang, C.; Holland, A.; Elefanty, A. G.; Stanley, E. G.; Greiner, D. L.; Keller, G. Efficient generation of NKX6-1+ pancreatic progenitors from multiple human pluripotent stem cell lines. *Stem Cell Rep.* **2015**, *4*, 591–604.

(46) Lehmann, R.; Lee, C. M.; Shugart, E. C.; Benedetti, M.; Charo, R. A.; Gartner, Z.; Hogan, B.; Knoblich, J.; Nelson, C. M.; Wilson, K. M. Human organoids: a new dimension in cell biology. *Mol. Biol. Cell* **2019**, *30*, 1129–1137.

(47) Cabrera, O.; Berman, D. M.; Kenyon, N. S.; Ricordi, C.; Berggren, P.-O.; Caicedo, A. The unique cytoarchitecture of human pancreatic islets has implications for islet cell function. *Proc. Natl. Acad. Sci. U. S. A.* **2006**, *103*, 2334–2339.

(48) Brereton, H. C.; Carvell, M. J.; Asare-Anane, H.; Roberts, G.; Christie, M. R.; Persaud, S. J.; Jones, P. M. Homotypic cell contact enhances insulin but not glucagon secretion. *Biochem. Biophys. Res. Commun.* **2006**, *344*, 995–1000.

(49) Crapo, P. M.; Gilbert, T. W.; Badylak, S. F. An overview of tissue and whole organ decellularization processes. *Biomaterials* **2011**, *32*, 3233–3243.

(50) Haque, M. A.; Nagaoka, M.; Hexig, B.; Akaike, T. Artificial extracellular matrix for embryonic stem cell cultures: a new frontier of nanobiomaterials. *Sci. Technol. Adv. Mater.* **2010**, *11*, 014106.

(51) Kibbey, M. C. Maintenance of the EHS sarcoma and Matrigel preparation. *J. Tissue Cult. Methods* **1994**, *16*, 227–230.

(52) Hughes, C. S.; Postovit, L. M.; Lajoie, G. A. Matrigel: a complex protein mixture required for optimal growth of cell culture. *Proteomics* **2010**, *10*, 1886–1890.

(53) Vigier, S.; Gagnon, H.; Bourgade, K.; Klarskov, K.; Fülop, T.; Vermette, P. Composition and organization of the pancreatic extracellular matrix by combined methods of immunohistochemistry, proteomics and scanning electron microscopy. *Curr. Res. Transl. Med.* **2017**, *65*, 31–39.

(54) De Carlo, E.; Baiguera, S.; Conconi, M. T.; Vigolo, S.; Grandi, C.; Lora, S.; Martini, C.; Maffei, P.; Tamagno, G.; Vettor, R.; Sicolo, N.; Parnigotto, P. P. Pancreatic acellular matrix supports islet survival and function in a synthetic tubular device: in vitro and in vivo studies. *Int. J. Mol. Med.* **2010**, *25*, 195–202.

(55) Berger, C.; Bjørlykke, Y.; Hahn, L.; Mühlemann, M.; Kress, S.; Walles, H.; Luxenhofer, R.; Ræder, H.; Metzger, M.; Zdzieblo, D. Matrix decoded - A pancreatic extracellular matrix with organ specific cues guiding human iPSC differentiation. *Biomaterials* **2020**, *244*, 119766.

(56) Johansson, K. A.; Dursun, U.; Jordan, N.; Gu, G.; Beermann, F.; Gradwohl, G.; Grapin-Botton, A. Temporal control of neurogenin3 activity in pancreas progenitors reveals competence windows for the generation of different endocrine cell types. *Dev. Cell* **2007**, *12*, 457–465.

(57) Kim, J. H.; Park, B. G.; Kim, S. K.; Lee, D. H.; Lee, G. G.; Kim, D. H.; et al. Nanotopographical regulation of pancreatic islet-like cluster formation from human pluripotent stem cells using a gradient-pattern chip. *Acta Biomater.* **2018**, *95*, 337–347.

(58) Shaer, A.; Azarpira, N.; Karimi, M. H.; Soleimani, M.; Dehghan, S. Differentiation of Human-Induced Pluripotent Stem Cells Into Insulin-Producing Clusters by MicroRNA-7. *Experimental and Clinical Transplantation* **2016**, *14*, 555–563.